

Characteristics of *Borrelia hermsii* infection in human hematopoietic stem cell-engrafted mice mirror those of human relapsing fever

Raja Vuyyuru, Hongqi Liu, Tim Manser¹, and Kishore R. Alugupalli¹

Department of Microbiology and Immunology, Kimmel Cancer Center, Thomas Jefferson University, Philadelphia, PA 19107

Edited* by Jeffrey V. Ravetch, The Rockefeller University, New York, NY, and approved November 14, 2011 (received for review June 13, 2011)

Rodents are natural reservoirs for a variety of species of *Borrelia* that cause relapsing fever (RF) in humans. The murine model of this disease recapitulates many of the clinical manifestations of the human disease and has revealed that T cell-independent antibody responses are required to resolve the bacteremic episodes. However, it is not clear whether such protective humoral responses are mounted in humans. We examined *Borrelia hermsii* infection in human hematopoietic stem cell-engrafted nonobese diabetic/SCID/IL-2R γ^{null} mice: "human immune system mice" (HISmice). Infection of these mice, which are severely deficient in lymphoid and myeloid compartments, with *B. hermsii* resulted in persistent bacteremia. In contrast, this infection in HISmice resulted in recurrent episodes of bacteremia, the hallmark of RF. The resolution of the primary episode of bacteremia was concurrent with the generation of *B. hermsii*-specific human IgM. Remarkably, HISmice generated antibody responses to the *B. hermsii* outer-membrane protein Factor H binding protein A. Sera from humans infected by *B. hermsii* have a similar reactivity, and studies in mice have shown that this response is generated by the B1b cell subset. HISmice contain several B-cell subsets, including those with the phenotype CD20⁺CD27⁺CD43⁺CD70⁻, a proposed human equivalent of mouse B1 cells. Reduction of B cells by administration of anti-human CD20 antibody resulted in diminished anti-*B. hermsii* responses and persistent bacteremia in HISmice. These data indicate that analysis of *B. hermsii* infection in HISmice will serve as a model in which to study the cellular and molecular mechanisms involved in controlling human RF.

B1 lymphocyte | splenomegaly | spirochete | antigenic variation

Relapsing fever (RF) in humans can be caused by arthropod-borne spirochetes of the genus *Borrelia* (1). This infection is characterized by febrile episodes of bacteremia, and it can extend to a variety of tissues (2–4). The major agents of RF in North America, *Borrelia hermsii* and *Borrelia turicatae*, are transmitted to humans by bites from infected ticks (5). Rodents are natural reservoirs of tick-borne RF *Borreliae* and the murine model of RF borreliosis recapitulates a number of pathophysiological aspects of the human disease (3, 6, 7).

The hallmark of this infection is recurrent episodes of high-level bacteremia (>10⁴ bacteria/ μ L blood), each caused by antigenically distinct populations of bacteria generated by rearrangements of the genes encoding the dominant outer surface antigen variable major proteins (Vmp) (8). Remarkably, each episode is resolved within a few days (9–11). T cell-independent B-cell responses are necessary and sufficient for clearing the RF bacteremia in mice (9, 11–13). Mice deficient only in the secretion of IgM experience persistently high bacteremia and become moribund. In contrast, activation-induced cytidine deaminase-deficient mice, which generate only IgM, control *B. hermsii* as efficiently as WT mice. These data demonstrate that IgM is necessary and sufficient for controlling *B. hermsii* in mice (11). Indeed, passive transfer of IgM from convalescent mice to naive mice is sufficient to confer protection (14, 15).

Four phenotypically and functionally distinct B-cell subsets have been described in mice: follicular (FO or B2), marginal zone (MZ), B1a, and B1b (16, 17). The latter three subsets can efficiently mount T cell-independent responses (16, 17). We have previously shown that mice deficient in B1a cells control infections by both the highly virulent *B. hermsii* strain DAHp-1 (which grows to >10⁴/ μ L blood) as well as an attenuated strain DAH-p19 (which was generated by serial in vitro passage of DAH-p1 and reaches \sim 10³/ μ L blood) (12). In contrast, concurrent with the resolution of DAHp-1 and DAH-p19 bacteremia, B1b cells in the peritoneal cavity expand and Rag1^{-/-} mice reconstituted with these B1b cells generate a *B. hermsii*-specific IgM response that is required for conferring long-lasting protection (11, 12). We found that the IgM-derived from B1b cells of convalescent mice recognizes a specific *B. hermsii* outer-membrane protein, Factor H binding protein A (FhbA), a putative virulence factor present on a majority of *B. hermsii* clinical isolates (18, 19). Inefficient clearance of DAH-p1 in splenectomized mice during the primary bacteremic episode suggests that MZ B cells also play a role in controlling *B. hermsii* during a heightened bacteremia (7, 11). Consistent with this, Bockenstedt and coworkers have demonstrated that MZ B cells mount anti-*B. hermsii* antibody responses (20).

These studies exemplify how mouse models have significantly contributed to our discovery of the immune mechanisms involved in the induction of protective immune responses to infectious pathogens. However, the relevance of findings made in murine models to an understanding of infectious disease progression and resolution in humans is often difficult to assess. Chimeric mice generated by xenografting severely immunodeficient mice such as nonobese diabetic Cg-Prkdc^{scid}/IL2r $\gamma^{\text{tm1Wjl/SzJ}}$ (NSG) mice with human hematopoietic stem cells (HSCs) provide an experimental platform to investigate this issue. Such xenograftment results in reconstitution of many compartments of the human immune system (21–23). As such, these mice can be referred to as "human immune system" mice (HISmice) (24–30). In the present study, we found that *B. hermsii* infection of HISmice mice results in recurrent episodes of bacteremia, the hallmark of this infection in humans. Moreover, resolution of this bacteremia was human B cell-dependent and correlated with the production of human IgM with specificities analogous to those observed in *B. hermsii*-infected mice and humans. As HISmice contain a variety of phenotypically distinct peripheral B-cell subsets, further analysis of this model should allow evaluation of whether one or several of these subsets are required for

Author contributions: R.V., T.M., and K.R.A. designed research; R.V., H.L., and K.R.A. performed research; R.V., T.M., and K.R.A. analyzed data; and T.M. and K.R.A. wrote the paper.

The authors declare no conflict of interest.

*This Direct Submission article had a prearranged editor.

¹To whom correspondence may be addressed. E-mail: manser@kimmelcancercenter.org or kishore.alugupalli@mail.jci.tju.edu.

This article contains supporting information online at www.pnas.org/lookup/suppl/doi:10.1073/pnas.1108776109/-DCSupplemental.

resistance to *B. hermsii* infection, as the B1b and MZ subsets are in the mouse.

Results

Recurrent Episodes of *B. hermsii* Bacteremia in HISmice. *B. hermsii* infection results in recurrent episodes of bacteremia in several inbred WT mouse models (31). Each episode consists of antigenically distinct populations of bacteria expressing different Vmps (32, 33). When WT mice are infected with strain DAH-p1 (which expresses Vmp2), the peak bacterial density during the primary episode can reach approximately 5×10^4 spirochetes/ μ L blood, and this episode lasts for 3 d (19). Typically, the subsequent relapses are significantly less severe, and by 3 to 4 wk postinfection, the bacteremic episodes are undetectable. NSG mice, similar to mice deficient in B cells (e.g., *scid*, *Rag1*^{-/-}, or μ MT^{-/-}) or IgM (sIgM^{-/-}) (11) experience persistently high levels of bacteremia (Fig. 1A, Middle). Unlike NSG mice, HISmice controlled the primary bacteremic episode by 7 to 9 d after infection (Fig. 1A, Bottom). However, the bacterial burden in HISmice was fivefold higher than that observed in WT mice. Similarly, although the second episode of bacteremia was more prolonged compared with WT mice (Fig. 1A), it was less severe than the primary episode in HISmice as well as in WT mice. Despite control of the initial waves of bacteremia, HISmice infected with DAH-p1 became moribund by 3 wk after infection.

HISmice Generate Anti-*B. hermsii* IgM Responses Concurrent with Resolution of Bacteremic Episodes. The anti-*B. hermsii* IgM response in WT mice occurs as early as 3 to 4 d after infection, and the generation of this response coincides with the resolution of the primary bacteremic episode (12). A delay in anti-*B. hermsii* responses typically results in more severe bacteremic episodes (31). Consistent with this, the severity of primary bacteremic episode in HISmice was associated with a delayed anti-*B. hermsii* human IgM response (Fig. 1B). WT mice mount a specific IgM response to FhbA, and B1b cells of immune mice can generate this response (19). As IgM or sera of patients with RF also recognize FhbA, in addition to a number of other proteins (18, 34), we tested whether HISmice also generate a response to this antigen. Immune HISmice contained serum IgM specific for FhbA, but at levels lower than that seen in immune WT mice (Fig. 1C).

HISmice Efficiently Control a Moderately Virulent Strain of *B. hermsii*.

Although HISmice controlled primary and secondary bacteremic episodes by the highly virulent strain DAH-p1, the duration and severity of these episodes were greater than that observed in WT C57BL6 mice (Fig. 1A), suggesting that the reconstitution of the B cells required for controlling *B. hermsii* in these mice is suboptimal. In WT mice, control of strain DAH-p1 but not strain DAH-p19 requires MZ B cells (11). As the existence of functional equivalents of MZ B cells in HISmice has not been described to our knowledge, we evaluated *B. hermsii* infection in HISmice by using DAH-p19. Infection of NSG mice with DAH-p19 resulted in persistent bacteremia more than two orders of magnitude higher than seen in WT mice (Fig. 2A). Although DAH-p19 caused heightened and prolonged bacteremic episodes in HISmice compared with WT mice, by 4 wk, bacteremia was controlled and the mice did not become moribund, unlike HISmice infected with strain DAH-p1. Moreover, these convalescent mice also generated anti-FhbA-specific IgM responses (Fig. 2B).

Analysis of B Cells in Spleen and Peritoneal Cavity of HISmice. Splenic B cells and peritoneal B cells, in particular the B1b cell subset, play a critical role in controlling *B. hermsii* in mice (11, 12). As HISmice control *B. hermsii* and mount a specific IgM response, we analyzed the composition of B cells in their spleens and peritoneal cavities, by using markers that identify various subsets of B cells in normal mice, as well as markers of maturity. A majority of B cells in the spleen expressed CD10, a marker of B-cell immaturity, but numerous IgM^{high}, IgD^{low} and IgD⁺, IgM⁺ CD10⁻ B cells were also present (Fig. S1).

Recently, a population of B cells (CD20⁺CD27⁺CD43⁻CD70⁻) was identified in human cord blood and adult peripheral blood that has properties characteristic of mouse B1 cells (35). Approximately 75% of these cells express CD5, suggesting that humans may contain both B1a (CD5⁺) and B1b (CD5⁻) cell subsets (35). We analyzed the peritoneal cavity and spleen of HISmice for the presence of B cells with this phenotype. We found that approximately 1% of the peritoneal compartment was comprised of CD19⁺ cells, of which approximately 30% were naive B cells (CD20⁺CD27⁻CD43⁻), approximately 30% were memory B cells (CD20⁺CD27⁺CD43⁻), and approximately 40% were CD20⁺CD27⁺CD43⁺CD70⁻ cells (Fig. 3A). In spleen, more than

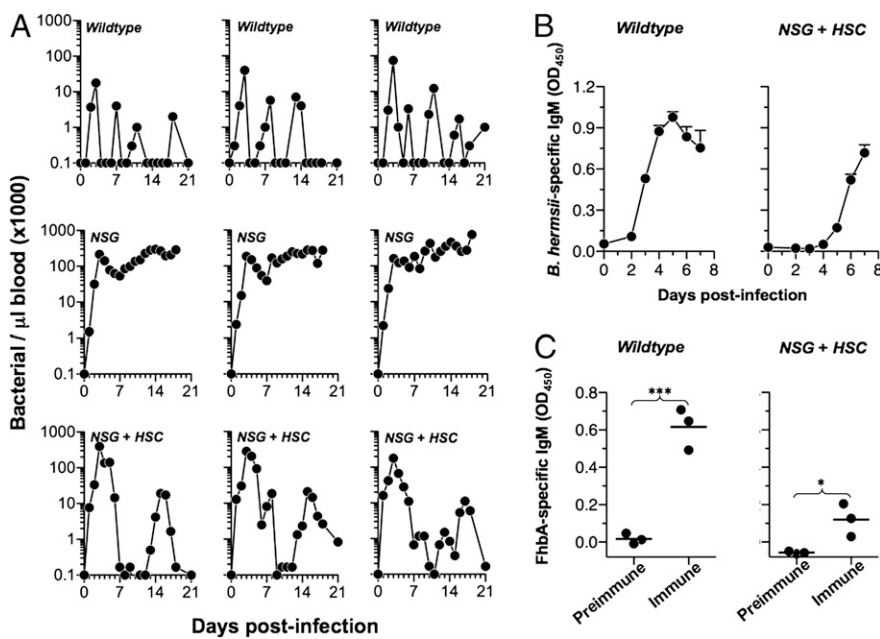


Fig. 1. HISmice can resolve severe bacteremic episodes and mount *B. hermsii*-specific IgM responses. (A) WT (C57BL/6), NSG, or human hematopoietic stem cell-engrafted NSG (NSG+HSC) mice were infected i.v. with 5×10^4 *B. hermsii* strain DAH-p1, and bacteremia was monitored by dark-field microscopy. Each plot represents data from an individual mouse. Representative data from three mice from a total of seven are shown (B) *B. hermsii*-specific IgM generated during an i.v. infection of WT (C57BL/6) or HISmice (NSG+HSC) was measured by ELISA. Mean \pm SD values are shown. (C) FhbA-specific IgM in preimmune (day 0 postinfection) or immune (1–3 wk postinfection) mice following i.v. infection was measured by ELISA. Data points represent individual animals, and horizontal bars represent means of each group. Statistical significance of genotype was measured by Student t test (*** $P < 0.001$ and * $P < 0.05$).

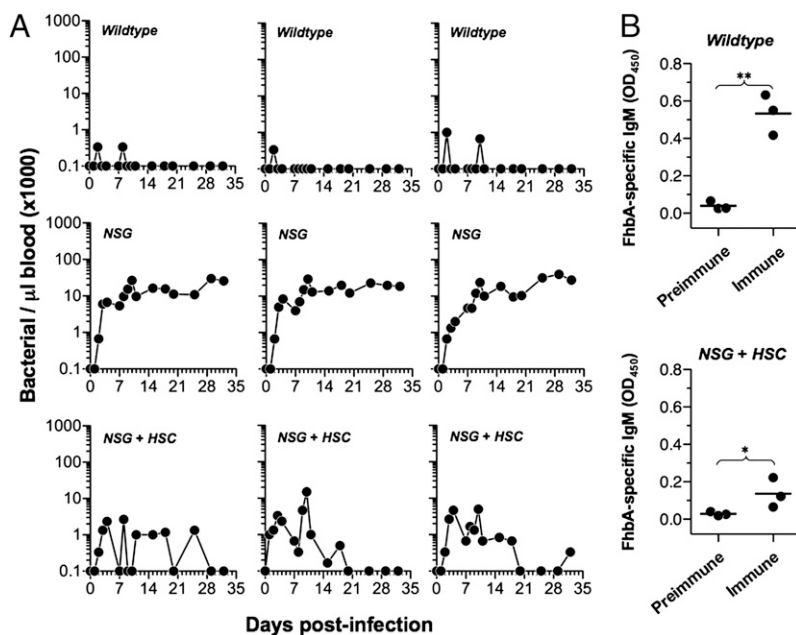


Fig. 2. Efficient resolution of moderate bacteremic episodes in HISmice. (A) WT (C57BL/6), NSG, or human hematopoietic stem cell-engrafted NSG (NSG+HSC) mice were infected intraperitoneally with 5×10^4 *B. hermsii* strain DAH-p19, and bacteremia was monitored by dark-field microscopy. Each plot represents data from an individual mouse. Representative data from three mice from a total of six are shown. (B) FhbA-specific IgM in preimmune (day 0 postinfection) or immune (1–3 wk postinfection) mice following i.p. infection was measured by ELISA. Data points represent individual animals, and horizontal bars represent means of each group. Statistical significance of genotype was measured by Student *t* test (**P* < 0.05 and ***P* < 0.01).

15% of the cells expressed CD19 and approximately 40% of them were naive B cells, approximately 5% were memory B cells, and the remainder had the human B1 phenotype (Fig. 3B). Blood contained approximately 1% CD19⁺ cells, and the phenotype and composition of these cells were comparable to the cells in the spleen (Fig. 3C). Although the majority of the “B1-like” cells in peritoneal cavity, spleen, and blood of HISmice expressed CD5, a fraction of them did not (Fig. 3A–C).

Histological analyses of spleens and mesenteric lymph nodes of HISmice revealed lymphoid-rich cell clusters in which T cells and B cells were partially segregated into distinct regions (Fig. 3D and E). However, the microarchitecture of these lymphoid regions was not as well demarcated as is characteristic of these organs in mice and humans. In addition, these analyses did not reveal a well defined MZ region containing IgM^{high}, IgD^{low} B cells, the phenotype of murine MZ B cells.

Depletion of B Cells in HISmice Results in Diminished Anti-*B. hermsii* Responses. T cell-independent B-cell responses are critical for controlling *B. hermsii*, and mice deficient in B cells or IgM are completely incapable of controlling *B. hermsii* (9–11). To determine if humoral responses are critical for protective immunity to *B. hermsii* in HISmice, we treated them with rituximab (anti-human CD20) before infection. This treatment resulted in reduction in B cells in the circulation as well as in peritoneal cavity and spleen (Fig. 4A). These B cell-depleted HISmice, when infected with *B. hermsii* DAH-p1, exhibited a severe impairment in anti-*B. hermsii* as well as anti-FhbA IgM responses (Fig. 4C and D), and suffered persistently high-level bacteremia that was comparable to that in NSG mice, and became moribund by 2 wk after infection (Fig. 4B).

Discussion

Rodent models have been exceptionally useful for elucidating the immunological mechanisms underlying protective responses to viral, bacterial, and parasitic infections. However, species-specific variation in immune responses to a given pathogen are common (24, 25, 27). This situation poses limitations on the degree to which findings made in rodent models can be translated to better understanding of immune responses to infectious pathogens in humans. In the present study, we have developed a model of *B. hermsii* infection in mice reconstituted with a human immune

system. This infection system recapitulates the hallmark of human RF - recurrent episodes of bacteremia. Furthermore, this infection induces specific IgM antibody responses that are observed in humans and mice (18, 34). *B. hermsii*-infected HISmice also exhibit splenomegaly, a characteristic found in humans as well as mice (Fig. S2). These findings suggest that HISmice will be a powerful experimental platform for use in testing the relevance of data obtained on the mechanisms of microbial pathogenesis and antimicrobial antibody responses in rodent models to an understanding of these processes in humans.

We found that the frequency of human B1 cells differentiated from human umbilical cord blood HSCs and the overall B-cell composition in HISmice is strikingly similar (Fig. 3) to that found in human umbilical cord blood (35). The frequency of B1 cells decreases with age in normal individuals (35), and therefore the high frequency of B1 cells that we have found in HISmice could be a result of the use of umbilical cord blood HSCs as opposed to adult human bone marrow HSCs in the generation of our HISmice. This also implies that our current human immune system mouse model likely represent that of the humoral immune system of human infants.

Although HISmice can control *B. hermsii* infection, they do so less efficiently than adult WT mice. Our data suggest that this may be caused by the relative immaturity of the B-cell compartment in these mice, a low frequency of a functional B-cell subset necessary for the anti-*B. hermsii* IgM response, or both. The murine cytokine environment may not be optimal for supporting development of mature human B cells. Indeed, expression of human cytokines in NSG mice was shown to enhance the efficiency of reconstitution of a variety of human immune compartments including dendritic cells, monocytes and macrophages, and NK cells (36). IL-7, a nonredundant cytokine for both B- and T-cell development in mice (37) enhances T-cell development in HISmice (38). Although its effect on B-cell development in HISmice has not been characterized, administration of human IL-7 might augment B-cell development quantitatively and qualitatively (39–41). For example, IL-7 was shown to increase B-cell receptor (BCR) diversity in mice (40), and IL-7-dependent murine B cells play an important role in generating a T cell-independent responses to a variety of antigens (42).

Another possibility for the suboptimal responses in HISmice to *B. hermsii* could be attributed to the source of HSCs used for

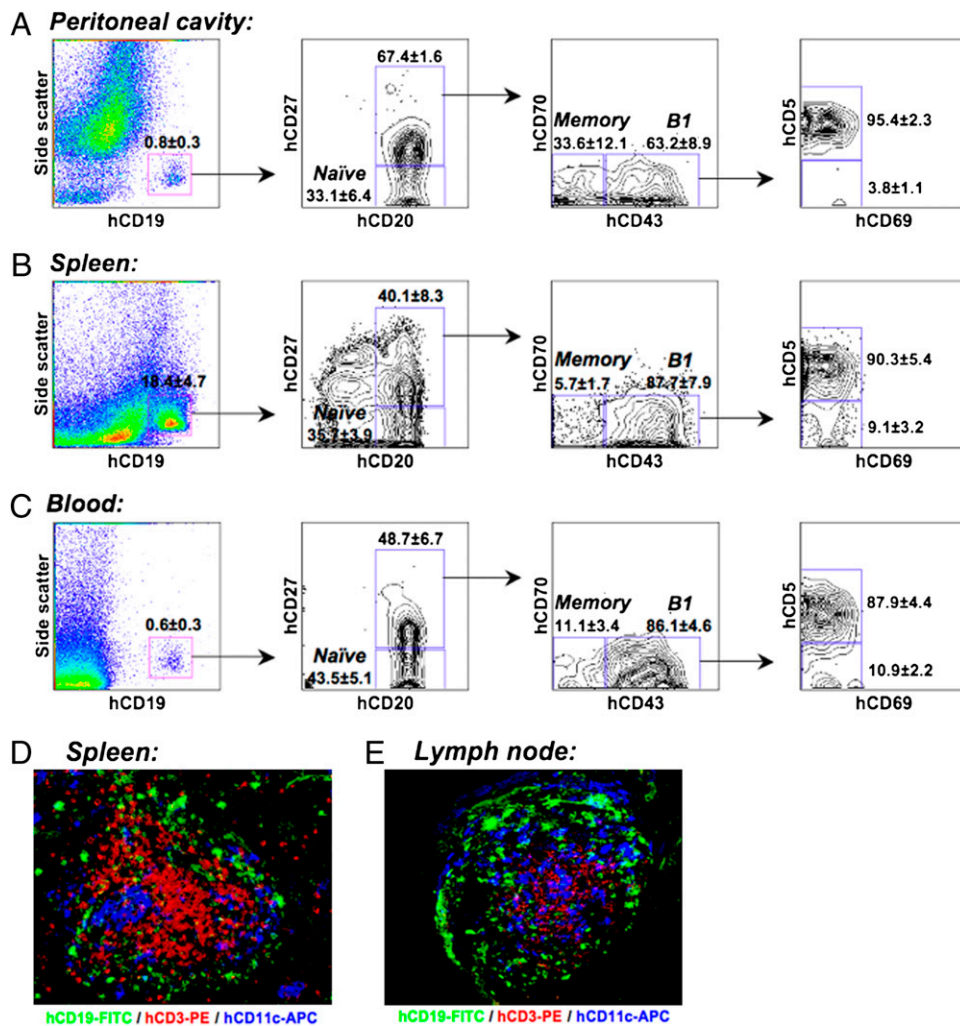


Fig. 3. Analysis of B cells in HISmice. (A) Peritoneal cavity cells, (B) spleen cells, and (C) blood were stained with antibodies specific for human CD19, CD20, CD27, CD43, CD70, and CD69, and analyzed by flow cytometry. All B cells were first identified by CD19 positivity and were further resolved (indicated by arrows) as naive ($CD20^+CD27^-$), memory B cells ($CD20^+CD27^+CD43^-CD70^-$), and B1 cells ($CD20^+CD27^+CD43^+CD70^-$). As described previously (35), a majority of these B1 cells expressed CD5. The frequency values of the indicated B-cell populations are shown within the plots. The data were generated by analyzing a minimum of 20,000 cells and are representative of three to five mice. Five percent contour plots are shown. Immunohistochemistry of (D) spleen and (E) mesenteric lymph nodes of a representative mouse.

reconstitution. Mouse B cells derived from fetal progenitors contain a high frequency of natural antibody-producing cells that have a restricted BCR repertoire (43, 44). Such cells are known to mount responses to evolutionarily conserved bacterial antigens such as phosphorylcholine (45), but not to structurally diverse antigens such as those expressed on a number of bacterial pathogens including *B. hermsii* (11, 46, 47). In contrast, murine B cells derived from adult precursors possess diverse BCR repertoires (48, 49). Comparison of HISmice reconstituted with HSCs derived from umbilical cord blood and adult bone marrow will be required to test this idea.

In the mouse system, *B. hermsii* infection induces expansion of a population of B1b cells that persists for extending periods after the infection is cleared and is responsible for resistance to reinfection. Neither expansion nor persistence of this population requires the presence of T cells, demonstrating that this is a unique T cell-independent form of immune memory. HISmice contain a subset of human B cells suggested to be the functional equivalents of murine B1 B cells, as well as several other B-cell subsets (35). As such, by applying experimental approaches developed in mouse models to improved versions of HISmice, it should be possible to determine which of these subsets are pivotal for resolution of *B. hermsii* bacteremia, whether the response of this subset is T cell-independent, and whether the responding human B cells give rise to an expanded, persistent population that confers long-lasting resistance to reinfection. It is likely that this general strategy will be of utility for elucidating

the molecular and cellular basis for antibody-mediated clearance of and immunity to a variety of human bacterial pathogens.

Materials and Methods

Mice. Mice were housed in microisolator cages with free access to food and water in a specific pathogen-free facility of Thomas Jefferson University. The studies were reviewed and approved by the institutional animal care and use committee. C57BL6/J and NSG mice were purchased from Jackson Laboratory and then bred in-house. The NSG mice were given sulfamethoxazole trimethoprim-containing drinking water on alternate weeks.

Isolation of CD34⁺ HSCs. Human cord blood was obtained from healthy full term newborns (Department of Obstetrics and Gynecology, Thomas Jefferson University) as approved by the institutional research board. After Ficoll gradient centrifugation to purify mononuclear cells, CD34⁺ cells were enriched by using immunomagnetic beads according to the manufacturer's instructions (CD34⁺ isolation kit; Miltenyi Biotec). The purity of isolated HSCs was more than 90% as evaluated by flow cytometry. Contaminating CD3⁺ T cell content was $0.9 \pm 1.5\%$. Cells were viably frozen in 90% FBS/10% DMSO at -150°C .

Xenotransplantation of HSCs into NSG Mice. Twenty-four to 48 h after birth, pups were given whole-body irradiation at a dose of 2 Gy (200 rad). After 4 h, 10^5 HSCs were injected intrahepatically in 25 μL of PBS solution by using a 30-gauge needle. Mice were weaned at 3 wk of age and randomly distributed among different experimental groups.

Flow Cytometry. To evaluate human immune cell engraftment, peripheral blood was collected into PBS solution containing 200 U of heparin/mL. Red blood cells were lysed and 0.1 to 1×10^6 cells were stained with appropriate

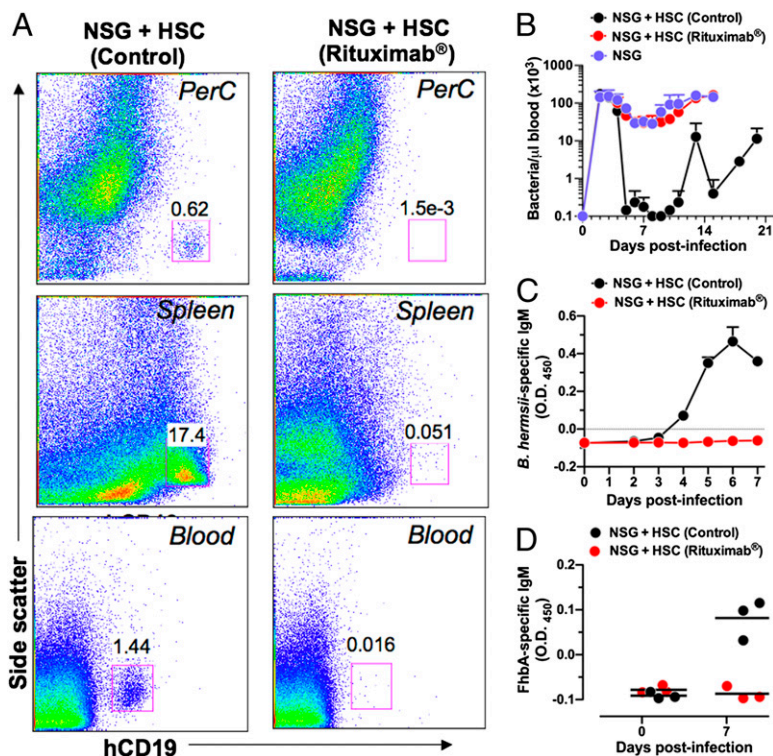


Fig. 4. Depletion of B cells results in impaired anti-*B. hermsii*-specific IgM responses and persistent bacteremia. (A) HISmice treated with ($n = 3$; rituximab) or without ($n = 3$; control) anti-human CD20 mAb and B-cell populations in peritoneal cavity, spleen, and blood were determined by flow cytometry using human CD19 antibodies. Representative FACS plot from one mouse is shown. Control or rituximab-treated mice were infected i.v. with *B. hermsii* DAH-p1 and (B) bacteremia, (C) anti-*B. hermsii*-specific IgM, and (D) anti-FhbA-specific IgM.

antibodies in 100 μ L of 1 \times PBS solution containing 3% BSA (Gemini Bio), 0.02% sodium azide, and 1 mM EDTA for 30 min on ice. The fraction of human hematopoiesis-derived cells was determined by anti-huCD45 staining. All mice used in experiments contained a proportion of at least 50% human CD45⁺ cells in peripheral blood lymphocytes. To determine the frequency of various B-cell populations, spleen and peritoneal cavity cells were harvested from individual mice in staining medium [deficient RPMI medium 1640 (Irvine Scientific) with 3% new calf serum, 1 mM EDTA]. After blocking the murine Fc receptors with 2.4G2 antibody and human Fc receptors with FC block, an aliquot of 50 μ L (10^6 cells) of cells was incubated in a microtiter plate with appropriately diluted antibody. The following additional fluorescent-conjugated monoclonal antibodies specific for the indicated human antigens were used: CD5-FITC (UCHT2), CD11b-APC (CBRM1/5), CD19-Pacific blue (Hib19), CD20-Pacific blue (2H7), CD43-APC (CD43-10G7), CD69-PE (FN50) conjugates (Biolegend); CD3-APC (S4.1), CD56-PE (MEM-188), and IgM-FITC conjugates (Invitrogen); CD70-FITC (K; 24), CD27-APC-H7 (M-T271), CD34-PE (8G12), CD3-PE (UCHT1), IgD-PE (IA6-2), CD4-Percp-cy5.5 (SK3), CD8-Percp-cy5.5 (SK1), CD27-percp-cy5.5 (M-T271) conjugates (BD Pharmingen); and CD19-PE-Cy7 (HIB19) from eBioscience. Stained cells were analyzed on LSRII flow cytometers (BD Biosciences). At least 20,000 events were acquired per sample and analyzed with FlowJo software (TreeStar).

Immunohistology. At 16 wk after HSC transplantation, spleens and inguinal and brachial lymph nodes were collected from reconstituted mice and frozen in Tissue-Tek Optimal Cutting Temperature compound (Sakura Finetek). Immunofluorescent staining was performed on 6- μ m tissue sections as described (50, 51). The following anti-human antigen antibodies were used: CD19-FITC (SJ25-C1; Southern Biotech), IgM-FITC (H15001; Invitrogen), Ki67-FITC (F7268, DAKO), and CD3-PE (SK7) and CD11c APC (S-HCL-3) (BD Pharmingen). The stained sections were analyzed by using fluorescence microscopy (DM 5000B; Leica Microsystems), and digital images were analyzed by using LAS AF 1.8.1 software from Leica Microsystems.

Depletion of B Cells. For B-cell depletion of HISmice, anti-hCD20 mAb (rituximab; Genentech) was used. Antibody was diluted in sterile PBS solution, and a dose of 40 μ g per mouse was injected i.v. twice per week for a total of 3 wk. The extent of B-cell depletion in peripheral blood, peritoneal cavity, and spleen was accessed by flow cytometry by using anti-human CD19 antibodies.

Infections. Twelve- to 16-wk-old mice were infected i.p. or i.v. via the tail vein with 5×10^4 bacteria of the fully virulent *B. hermsii* strain DAH-p1 (from the blood of an infected mouse) or DAH-p19, an attenuated strain derived from in vitro passing of DAH-p1. Blood bacteremia was monitored by dark-field microscopy (52).

ELISA. Murine IgM responses were measured with ELISA kits according to the manufacturer's instructions (Bethyl Laboratories). *B. hermsii*-specific murine or human IgM was measured by coating 96-well plates (ICN Biomedicals) with in vivo-grown *B. hermsii* DAH-p1 (10^5 wet bacteria per well). FhbA-specific IgM was measured by coating 96-well plates with 1 μ g/mL recombinant FhbA (19). All plates were washed and blocked with 2% BSA in PBS solution, pH 7.2, for 2 h at room temperature before use. Blood samples of immunized mice were diluted 1:125 (HISmice) or 1:250 (WT mice), the samples were centrifuged (16,000 \times g for 10 min), and the supernatant was used. Bound IgM was measured by using HRP conjugates of goat anti-mouse IgM or goat anti-human IgM.

Statistics. Statistical analysis was carried out using GraphPad Prism version 4 (GraphPad). Differences between control and infected groups were evaluated by Student *t* test (two tailed, unpaired), and a *P* value lower than 0.05 was deemed significant.

ACKNOWLEDGMENTS. This work was supported by National Institutes of Health Grants U19 AI 082726 (pilot project; to T.M.) and R01 AI065750 (to K.R.A.).

1. Southern PM, Jr., Sanford JP (1969) Relapsing fever: A clinical and microbiological review. *Medicine* 48:129–149.
2. Cadavid D, Barbour AG (1998) Neuroborreliosis during relapsing fever: Review of the clinical manifestations, pathology, and treatment of infections in humans and experimental animals. *Clin Infect Dis* 26:151–164.
3. Gebbia JA, Monco JC, Degen JL, Bugge TH, Benach JL (1999) The plasminogen activation system enhances brain and heart invasion in murine relapsing fever borreliosis. *J Clin Invest* 103:81–87.

4. Nordstrand A, Shamaei-Tousi A, Ny A, Bergström S (2001) Delayed invasion of the kidney and brain by *Borrelia crocidurae* in plasminogen-deficient mice. *Infect Immun* 69:5832–5839.
5. Burgdorfer W (1976) The epidemiology of the relapsing fevers. *The Biology of Parasitic Spirochetes*, ed Johnson RC (Academic, New York), pp 191–200.
6. Cadavid D, Thomas DD, Crawley R, Barbour AG (1994) Variability of a bacterial surface protein and disease expression in a possible mouse model of systemic Lyme borreliosis. *J Exp Med* 179:631–642.

7. Alugupalli KR, et al. (2003) Spirochete-platelet attachment and thrombocytopenia in murine relapsing fever borreliosis. *Blood* 102:2843–2850.
8. Barbour AG (1990) Antigenic variation of a relapsing fever *Borrelia* species. *Annu Rev Microbiol* 44:155–171.
9. Barbour AG, Bundoc V (2001) In vitro and in vivo neutralization of the relapsing fever agent *Borrelia hermsii* with serotype-specific immunoglobulin M antibodies. *Infect Immun* 69:1009–1015.
10. Connolly SE, Benach JL (2001) Cutting edge: The spirochetemia of murine relapsing fever is cleared by complement-independent bactericidal antibodies. *J Immunol* 167:3029–3032.
11. Alugupalli KR, et al. (2003) The resolution of relapsing fever borreliosis requires IgM and is concurrent with expansion of B1b lymphocytes. *J Immunol* 170:3819–3827.
12. Alugupalli KR, et al. (2004) B1b lymphocytes confer T cell-independent long-lasting immunity. *Immunity* 21:379–390.
13. Connolly SE, Benach JL (2005) The versatile roles of antibodies in *Borrelia* infections. *Nat Rev Microbiol* 3:411–420.
14. Arimitsu Y, Akama K (1973) Characterization of protective antibodies produced in mice infected with *Borrelia duttonii*. *Jpn J Med Sci Biol* 26:229–237.
15. Yokota M, Morshed MG, Nakazawa T, Konishi H (1997) Protective activity of *Borrelia duttonii*-specific immunoglobulin subclasses in mice. *J Med Microbiol* 46:675–680.
16. Martin F, Kearney JF (2001) B1 cells: Similarities and differences with other B cell subsets. *Curr Opin Immunol* 13:195–201.
17. Alugupalli KR (2008) A distinct role for B1b lymphocytes in T cell-independent immunity. *Curr Top Microbiol Immunol* 319:105–130.
18. Hovis KM, Schriefer ME, Bahlani S, Marconi RT (2006) Immunological and molecular analyses of the *Borrelia hermsii* factor H and factor H-like protein 1 binding protein, FhbA: Demonstration of its utility as a diagnostic marker and epidemiological tool for tick-borne relapsing fever. *Infect Immun* 74:4519–4529.
19. Colombo MJ, Alugupalli KR (2008) Complement factor H-binding protein, a putative virulence determinant of *Borrelia hermsii*, is an antigenic target for protective B1b lymphocytes. *J Immunol* 180:4858–4864.
20. Belperron AA, Dailey CM, Bockenstedt LK (2005) Infection-induced marginal zone B cell production of *Borrelia hermsii*-specific antibody is impaired in the absence of CD1d. *J Immunol* 174:5681–5686.
21. Brehm MA, Shultz LD, Greiner DL (2010) Humanized mouse models to study human diseases. *Curr Opin Endocrinol Diabetes Obes* 17:120–125.
22. Shultz LD, Ishikawa F, Greiner DL (2007) Humanized mice in translational biomedical research. *Nat Rev Immunol* 7:118–130.
23. Pearson T, Greiner DL, Shultz LD (2008) Humanized SCID mouse models for biomedical research. *Curr Top Microbiol Immunol* 324:25–51.
24. Libby SJ, et al. (2010) Humanized nonobese diabetic-scid IL2rgamma null mice are susceptible to lethal *Salmonella Typhi* infection. *Proc Natl Acad Sci USA* 107:15589–15594.
25. Jaiswal S, et al. (2009) Dengue virus infection and virus-specific HLA-A2 restricted immune responses in humanized NOD-scid IL2rgamma null mice. *PLoS ONE* 4:e7251.
26. King M, Pearson T, Rossini AA, Shultz LD, Greiner DL (2008) Humanized mice for the study of type 1 diabetes and beta cell function. *Ann N Y Acad Sci* 1150:46–53.
27. Kumar P, et al. (2008) T cell-specific siRNA delivery suppresses HIV-1 infection in humanized mice. *Cell* 134:577–586.
28. Mota J, Rico-Hesse R (2009) Humanized mice show clinical signs of dengue fever according to infecting virus genotype. *J Virol* 83:8638–8645.
29. Tonomura N, Habiro K, Shimizu A, Sykes M, Yang YG (2008) Antigen-specific human T-cell responses and T cell-dependent production of human antibodies in a humanized mouse model. *Blood* 111:4293–4296.
30. Shacklett BL (2008) Can the new humanized mouse model give HIV research a boost. *PLoS Med* 5:e13.
31. Alugupalli KR, Akira S, Lien E, Leong JM (2007) MyD88- and Bruton's tyrosine kinase-mediated signals are essential for T cell-independent pathogen-specific IgM responses. *J Immunol* 178:3740–3749.
32. Barbour AG, Tessier SL, Stoenner HG (1982) Variable major proteins of *Borrelia hermsii*. *J Exp Med* 156:1312–1324.
33. Stoenner HG, Dodd T, Larsen C (1982) Antigenic variation of *Borrelia hermsii*. *J Exp Med* 156:1297–1311.
34. Lopez JE, et al. (2009) Identification of conserved antigens for early serodiagnosis of relapsing fever *Borrelia*. *Microbiology* 155:2641–2651.
35. Griffin DO, Holodick NE, Rothstein TL (2011) Human B1 cells in umbilical cord and adult peripheral blood express the novel phenotype CD20+ CD27+ CD43+ CD70-. *J Exp Med* 208:67–80.
36. Chen Q, Khoury M, Chen J (2009) Expression of human cytokines dramatically improves reconstitution of specific human-blood lineage cells in humanized mice. *Proc Natl Acad Sci USA* 106:21783–21788.
37. von Freeden-Jeffrey U, et al. (1995) Lymphopenia in interleukin (IL)-7 gene-deleted mice identifies IL-7 as a nonredundant cytokine. *J Exp Med* 181:1519–1526.
38. van Lent AU, et al. (2009) IL-7 enhances thymic human T cell development in "human immune system" Rag2-/-IL2Rgamma-/- mice without affecting peripheral T cell homeostasis. *J Immunol* 183:7645–7655.
39. Corcoran AE, Riddell A, Krooshoop D, Venkitaraman AR (1998) Impaired immunoglobulin gene rearrangement in mice lacking the IL-7 receptor. *Nature* 391:904–907.
40. Corcoran AE, et al. (1996) The interleukin-7 receptor alpha chain transmits distinct signals for proliferation and differentiation during B lymphopoiesis. *EMBO J* 15:1924–1932.
41. Erlandsson L, et al. (2004) Impaired B-1 and B-2 B cell development and atypical splenic B cell structures in IL-7 receptor-deficient mice. *Eur J Immunol* 34:3595–3603.
42. Shriner AK, Liu H, Sun G, Guimond M, Alugupalli KR (2010) IL-7-dependent B lymphocytes are essential for the anti-polysaccharide response and protective immunity to *Streptococcus pneumoniae*. *J Immunol* 185:525–531.
43. Kantor AB, Merrill CE, Herzenberg LA, Hillson JL (1997) An unbiased analysis of V(H)-D-J(H) sequences from B-1a, B-1b, and conventional B cells. *J Immunol* 158:1175–1186.
44. Tornberg UC, Holmberg D (1995) B-1a, B-1b and B-2 B cells display unique VHDJH repertoires formed at different stages of ontogeny and under different selection pressures. *EMBO J* 14:1680–1689.
45. Martin F, Kearney JF (2000) B-cell subsets and the mature preimmune repertoire. Marginal zone and B1 B cells as part of a "natural immune memory". *Immunol Rev* 175:70–79.
46. Gil-Cruz C, et al. (2009) The porin OmpD from nontyphoidal *Salmonella* is a key target for a protective B1b cell antibody response. *Proc Natl Acad Sci USA* 106:9803–9808.
47. Haas KM, Poe JC, Steeber DA, Tedder TF (2005) B-1a and B-1b cells exhibit distinct developmental requirements and have unique functional roles in innate and adaptive immunity to *S. pneumoniae*. *Immunity* 23:7–18.
48. Jeong HD, Teale JM (1988) Comparison of the fetal and adult functional B cell repertoires by analysis of VH gene family expression. *J Exp Med* 168:589–603.
49. Malynn BA, Yancopoulos GD, Barth JE, Bona CA, Alt FW (1990) Biased expression of JH-proximal VH genes occurs in the newly generated repertoire of neonatal and adult mice. *J Exp Med* 171:843–859.
50. Vora KA, et al. (1999) Severe attenuation of the B cell immune response in Msh2-deficient mice. *J Exp Med* 189:471–482.
51. Rahman ZS, Rao SP, Kalled SL, Manser T (2003) Normal induction but attenuated progression of germinal center responses in BAFF and BAFF-R signaling-deficient mice. *J Exp Med* 198:1157–1169.
52. Alugupalli KR, et al. (2001) Platelet activation by a relapsing fever spirochaete results in enhanced bacterium-platelet interaction via integrin alphaIIb beta3 activation. *Mol Microbiol* 39:330–340.